NACA RM L58E22

NACA

RESEARCH MEMORANDUM

QUALITATIVE MEASUREMENTS OF THE EFFECTIVE HEATS OF ABLATION OF SEVERAL MATERIALS IN SUPERSONIC AIR JETS AT STAGNATION TEMPERATURES UP TO 11,000° F

By Bernard Rashis, William G. Witte, and Russell N. Hopko

Langley Aeronautical Laboratory
Langley Field, Va.

NATIONAL ADVISORY COMMITTEE
FOR AERONAUTICS
WASHINGTON

July 7, 1958
Declassified December 1, 1959

NATIONAL ADVISORY COMMITTEE FOR AERONAUTICS

RESEARCH MEMORANDUM

QUALITATIVE MEASUREMENTS OF THE EFFECTIVE HEATS OF ABLATION OF SEVERAL MATERIALS IN SUPERSONIC AIR JETS AT STAGNATION TEMPERATURES UP TO 11,000° F *

By Bernard Rashis, William G. Witte, and Russell N. Hopko

SUMMARY

The effective heats of ablation of a number of materials were derived from tests in supersonic air jets at stagnation temperatures ranging from 2,000° F to 11,000° F. The materials included the plastics Teflon, nylon, Lucite, and polystyrene; the inorganic salts ammonium chloride and sodium carbonate, several phenolic resins of varied resin content and type of reinforcement; and a melamine-fiber glass laminate.

The results indicate that the effective heats of ablation range from 7 to 40 times greater than the heat-absorption capabilities of copper not undergoing ablation at the conditions tested. The effective heats of ablation for Teflon, nylon, and Rocketon, which were tested in both a ceramic-heated and an electric-arc-jet, increased with increasing aerodynamic heat flux. For several glass-reinforced phenolic-resin models, the resin content of which varied from 27 percent to 65 percent, the effective heats of ablation, for the same aerodynamic heat fluxes, decreased with increased resin content.

The inorganic salts, ammonium chloride and sodium carbonate, from which models were constructed by cold-pressing of crystals, did not compare well with the other materials with regard to strength; however, these models did show the highest values of effective heat of ablation at comparable aerodynamic heat fluxes in comparison with the other materials tested.

---

*Title, Unclassified.

INTRODUCTION

In order to reduce dispersion error due to winds and density variations for long-range ballistic missiles, consideration is being given to configurations with high weight-drag ratios. This requirement greatly intensifies the heating problem, the heat inputs to the nose being almost 20 times greater than for subsonic impact. These heating rates are of such magnitude that the heat-flux inputs which the nose-cone material must absorb are almost 40 times greater than those which conventional materials such as copper can withstand, as indicated by the analysis of reference 1, which takes into account the temperature gradient through the material.

Previous investigations of this problem by the Langley Pilotless Aircraft Research Division have involved the study of transpiration cooling (ref. 2), endothermic decomposition (ref. 3), upstream ejection of water (ref. 4), upstream ejection of solids (ref. 5), and radiation, latent heat of fusion, pyrolysis, and ablation (ref. 6). All these schemes may be considered as a means of increasing the effective heat capacity of the nose shape. The purpose of this paper is to present some qualitative measurements of the effective heat-absorption capacities of a number of materials undergoing ablation. The tests were conducted in a ceramic-heated jet of the Langley Pilotless Aircraft Research Division and an electric-arc-powered air jet of the Langley Structures Research Division at a nominal Mach number of 2.0.

SYMBOLS

A	surface area of nose shape, sq ft
$C_{p,g}$	specific heat of gas layer, Btu/lb-$^{\circ}$F
D	diameter of nose shape, ft
h	heat-transfer coefficient, Btu/(sq ft)(sec)($^{\circ}$F)
h_{eff}	effective heat of ablation, Btu/lb
H_e	boundary-layer-recovery enthalpy, Btu/lb
H_t	stagnation specific enthalpy, Btu/lb
H_g	gas-layer specific enthalpy, Btu/lb

$\bar{q}$ average heat flux to nose shape, Btu/(sq ft)(sec)

q_t stagnation heat flux, Btu/(sq ft)(sec)

T_t stagnation temperature, $^{\circ}F$

T_w surface temperature, $^{\circ}F$

$\dot{w}$ average nose-shape ablation rate, lb/sec

$\frac{\dot{w}}{A}$ average unit-area nose-shape ablation rate, lb/(sq ft)(sec)

GENERAL CONSIDERATIONS

In figure 1, there are shown schematic drawings of bodies undergoing two types of ablation: In figure 1(a) the body first melts forming a relatively thin layer of molten material or a liquid film which is then vaporized, the vaporized material forming a relatively thick gas layer; this process is hereinafter referred to as ablation by melting and vaporization. In figure 1(b) the body is directly vaporized, the vaporized material also forming a relatively thick gas layer; this process is hereinafter referred to as ablation by sublimation. All the materials investigated underwent ablation in one of these two ways. References 7 and 8 give detailed mathematical explanations of the mechanism of ablation by melting and vaporization. A brief discussion of the ablation mechanism as described in these references is given in the following paragraphs without resort to mathematical analysis. A brief discussion is also given of ablation by sublimation.

The following schematic diagram shows the heat flux for both types of ablation:

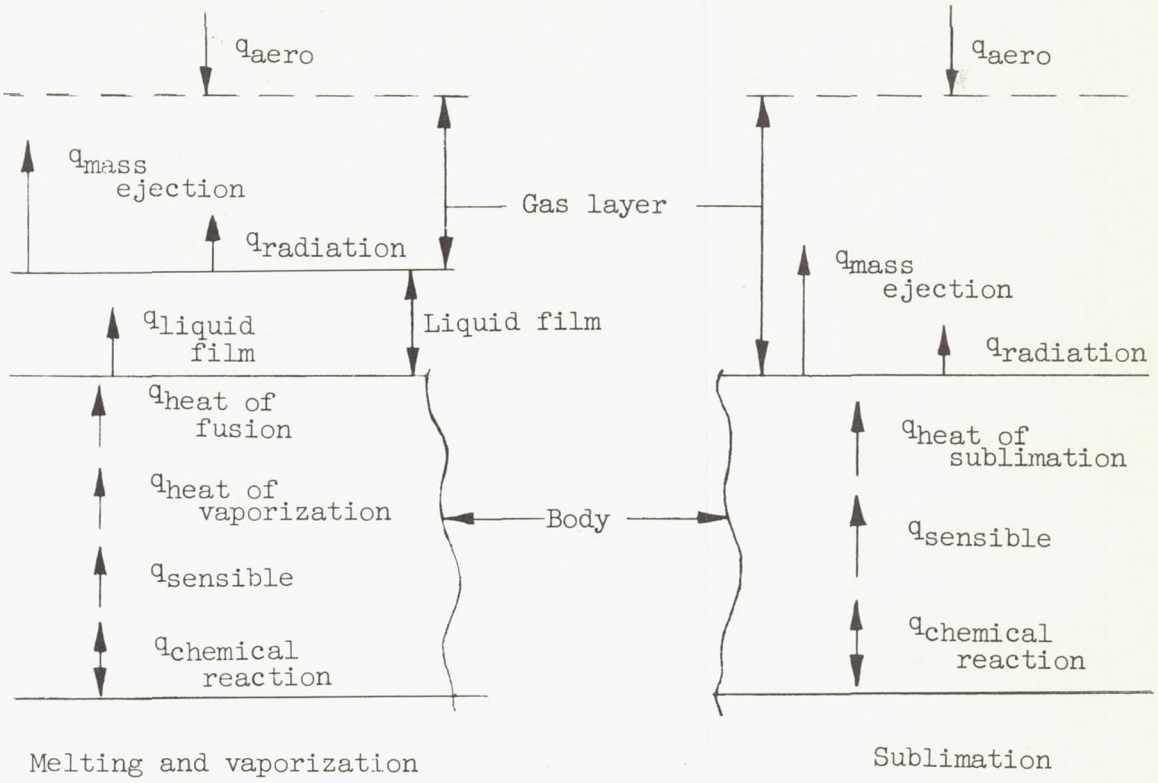

Melting and vaporization

Sublimation

For ablation by melting and vaporization, the general heat-balance equation is

$$q_{aero} \pm q_{chemical\ reaction} - \left(q_{mass\ ejection} + q_{liquid\ film} + q_{heat\ of\ fusion} + q_{heat\ of\ vaporization} + q_{sensible} + q_{radiation}\right) = 0$$

For ablation by sublimation, the general heat-balance equation is

$$q_{aero} \pm q_{\substack{chemical\\reaction}} - \left(q_{\substack{mass\\ejection}} + q_{\substack{heat\ of\\sublimation}} + q_{sensible} + q_{radiation}\right) = 0$$

The term q_{aero} is the aerodynamic heating due to the movement of the airstream over the body and the temperature difference between the airstream and the nose-shape surface. The term $q_{\substack{chemical\\reaction}}$ is the heating due to the reaction of the body material with the hot airstream. The term $q_{\substack{liquid\\film}}$ is the heat which is absorbed by the liquid film. The liquid film is moved downstream by the drag exerted on it by the boundary layer; thus, heat is picked up at the stagnation point and moved rearward. A result of the detailed analysis of reference 8 is that the liquid film is capable of blocking 30 percent of the heat flux into the liquid film from reaching the nonflowing solid interior for the specific case analyzed. The terms $q_{\substack{heat\ of\\fusion}}$ and $q_{\substack{heat\ of\\vaporization}}$ are the heats absorbed in melting or vaporizing the material undergoing ablation. The term $q_{sensible}$ is the heat which is absorbed by the ablated material in being raised from its initial temperature to the melting temperature in ablation by melting and vaporization and to the sublimation temperature in ablation by sublimation. The term $q_{radiation}$ is the heat emitted from the body by radiation.

For both cases, the predominate term is $q_{\substack{mass\\ejection}}$, which is the heat that has been blocked by the gas layer. A simple physical picture of how this blocking is achieved is obtained by considering the hot airstream as having a specific enthalpy H_t and the ejected gas as having a specific enthalpy H_g which is much less than H_t. Assuming that all of the ejected gas mixes with the hot airstream, a gas layer is formed over the body which is at a specific enthalpy level H_e. The value of H_e is greater than H_g but is less than H_t. The effect of mass ejection thus reduces the specific enthalpy level of the boundary layer. In addition, the ejected gas has absorbed the quantity of heat $(H_e - H_g)$. Since the heat input to the body depends on the enthalpy or temperature difference between the boundary layer and the body surface, the ejected gas has been of twofold action in blocking heat that would have gone into the body material. This twofold action accounts for the fact that the shielding or blocking effect increases nonlinearly with the aerodynamic

heat input. As a consequence, the term $q_{\substack{mass \\ ejection}}$ tends to predominate at high values of aerodynamic heat flux. This explanation has considered only first-order effects. In actuality, the mass-ejection mechanism is very complex.

It should be noted that the ablation mechanism acts in the direction that tends to keep the surface temperature relatively constant over wide ranges of q_{aero}. It is thus deduced that in ablation by melting and vaporization an increase in q_{aero} will show up essentially as a decrease in the thickness of the liquid film more so than as an increase in the surface temperature. In ablation by sublimation an increase in q_{aero} will show up as an increase in the enthalpy difference across the gas layer much more so than as an increase in the surface temperature.

It should not be inferred that since ablation by melting and vaporization has an additional heat-absorbing term it is a more effective method than ablation by sublimation. In ablation by melting and vaporization the term $q_{\substack{mass \\ ejection}}$ is evaluated for only the amount of the ablated material which is vaporized, which may be a small fraction of the melted material. In ablation by sublimation all of the ablated material is ejected into the boundary layer, and $q_{\substack{mass \\ ejection}}$ may be considerably larger than for ablation by melting and vaporization.

TEST FACILITY AND TEST MODELS

The ceramic-heated jet (laboratory model) and the electric-arc-powered air jet were utilized for the present tests. Reference 9 gives some of the details of construction and operation of these two facilities. Several preliminary tests, conducted in the ceramic-heated jet, were made of models having configurations B and D shown in figure 2. The basic configurations A and C (fig. 2) were adapted for the remainder of the tests conducted in the ceramic-heated jet. Configuration E (fig. 2) was tested in the electric-arc-powered air jet. Only the materials Teflon, nylon, and Rocketon were used for this configuration.

The Teflon, Lucite, nylon, polystyrene, Rocketon, and Planeton models were machined to size from commerically obtained materials. The ammonium chloride and sodium carbonate models were machined to size from rods formed by cold-pressing commerically obtained crystals. One-half-inch-diameter phenolic-resin models were machined from one-half-inch-diameter rods supplied by the Cincinnati Testing Laboratory; these rods

were all of high-temperature phenolic resin no. 37-9-X, but varied in percent of resin content and reinforcement material. The preliminary test models of configuration D were machined from commercially obtained reinforced phenolic and melamine resin rods. The Haveg Rocketon and Planeton materials are similar in composition to the phenolic-resin materials.

For all the tests conducted in the ceramic-heated jet, the jet exit Mach number was approximately 2.0 and the exit pressure was maintained at approximately sea-level pressure. The models were mounted on a side-injection-type sting and were inserted into the stream only after the required flow conditions were established. A timer which was synchronized with the sting was visually recorded along with the model for all the tests by high-speed motion-picture cameras. For the ceramic-heated jet, the stagnation temperatures were determined from calibrated pyrometer readings of the top surface of the heated ceramic bed. For the electric-arc-powered air jet the stagnation temperature (11,000° F) was determined from a calculation based on the measured jet static temperature which was observed with a spectroscope.

The surface temperatures of the models were not measured during the tests. The values used in the calculations were obtained from static test measurements of the melting temperatures for all the materials which exhibited a liquid film. In later tests, the surface temperatures were measured by an optical pyrometer while the models were undergoing ablation. The values obtained by this method were in agreement with the values previously assumed from the static tests. The sublimation and melting temperatures given in reference 10 were used for the ammonium chloride and sodium carbonate, respectively. The Teflon does not have a definite sublimation temperature; however, a survey of the available literature on Teflon indicated that a surface temperature of 1,000° F would be reasonable for the present tests. In table I there are listed the densities, thermal conductivities, and the specific heats of most of the materials tested. A list of all the materials tested is given in table II.

DATA REDUCTION

The ablation rates of the various materials were determined by two methods. One method involved the weighing, on an analytical balance, of the models before and after testing. The other method involved measuring the velocity at which the stagnation point receded from enlargements of high-speed motion-picture film. The best results with regard to sharpness and clarity of detail were obtained when the 16-millimeter motion-picture film was magnified 25 times. An arc was

then fitted to the nose contour and the radius of this arc was used in the calculation of the volume and the heat-transfer coefficient. Both methods checked except in the case of Teflon, which has a relatively large expansion when heated. In all cases, the motion pictures indicated that after a certain time had elapsed, the velocity at which the stagnation point receded was constant with time.

The average aerodynamic heat input into the nose shape was computed for the air-jet tests from

$$\bar{q} = 0.5q_t = 0.5\left[\frac{(h\sqrt{D})}{\sqrt{D}}(T_t - T_w)\right] \tag{1}$$

where the values of $(h\sqrt{D})$ were taken from the curve of figure 3(a), which was taken from reference 11. The constant 0.5 is the ratio of the average heat flux for the entire nose to that at the stagnation point, assuming laminar flow over the nose shape. Laminar heating was assumed since the Reynolds numbers of the tests based on model diameters were less than 60,000. The Mach number, static-pressure, velocity, and static-temperature ranges in the ceramic-heated jet are also given in figure 3.

For tests in the electric-arc-powered air jet the heat flux at the stagnation point was determined from a calorimeter model to be approximately 3,140 Btu/(sq ft)(sec). The average heat flux was assumed to be one-half this value or 1,570 Btu/(sq ft)(sec).

The effective heat of ablation was computed from

$$h_{eff} = \frac{\bar{q}}{\dot{w}/A} \tag{2}$$

where A is the surface area of the nose shape. The weight-loss values were corrected for extraneous losses from the model sides and the values of D and A were averaged to account for the slight changes in dimensions which occurred during the tests.

RESULTS AND DISCUSSION

In figure 4 there are shown the average ablation rates per unit area as a function of the average aerodynamic heat flux for Teflon, nylon, and Rocketon. It is clearly indicated from figure 4 that the

ablation rates determined from the tests in the arc jet are considerably lower than those that would be indicated by a linear extrapolation of the values obtained in the ceramic-heated jet. Since the diameters of the models tested in the two jets, as well as the test conditions, were different, it cannot be assumed that $\overline{q}$ alone is the correlating parameter; however, the marked dependence of the ablation rates upon $\overline{q}$ certainly establishes it as a parameter of primary importance.

In figure 5 there is shown the variation of h_{eff} with $\overline{q}$ for the data shown in figure 4. It should be noted that the values of h_{eff} obtained from tests in the arc jet are approximately two to three times greater than the values of h_{eff} corresponding to the highest value of $\overline{q}$ for the tests in the ceramic-heated jet. Although the Teflon indicates a rather high value of h_{eff} for the lowest heating rate, it is felt that the results at low heating rates are influenced somewhat by conduction into the solid and hence do not reflect values of effectiveness for steady ablation. This conduction effect was investigated experimentally for the Teflon by testing a series of models at approximately constant heating rate ($\overline{q}$ = 68 Btu/ft^2-sec) for successively longer periods of test time. The results shown in figure 6 indicate that the ablation rates rise sharply and then level off. Only the steady value was utilized for the results presented herein. The resulting error due to this finite time requirement to obtain steady ablation is about 10 percent; application of a correction for this error to the h_{eff} value of 3,100 Btu/lb at $\overline{q}$ = 76 Btu/(sq ft)(sec) results in the corrected value of h_{eff} = 2,830 Btu/lb.

Although the results shown in figure 5 have a small conduction error, it should be noted that the materials tested may very well be affected by conduction under prolonged low heating rates. For comparison purposes the calculated useful heat capacity of a copper heat sink (ref. 1) is shown.

In figure 7 there is shown the variation of the effective heat of ablation with resin content for two values of $\overline{q}$ for the 1/2-inch-diameter glass-reinforced phenolic-resin models. The results indicate that the value of h_{eff} decreases with increasing phenolic-resin content. The heat liberated from the reaction of the resin with the hot stream increases with the increasing resin content. At the higher heat condition the percentage effect of the burning decreases.

In table II, there is given a summary of all the test conditions. Except for Teflon, nylon, and Rocketon, for which arc-jet tests were conducted, all the tests were conducted in the ceramic-heated jet at values of $\overline{q}$ ranging from 70 to approximately 250 Btu/(sq ft)(sec). It

is of interest, however, to note that the inorganic salts indicated relatively high values of h_{eff} as compared with the other materials. Also, the models having configuration D (fig. 2), which were machined from commercial materials, indicate an increase in h_{eff} with finer mesh fiber glass reinforcement. Since the finer mesh model probably had a smaller percent of resin content, the results are probably affected in the same manner as the 1/2-inch-diameter resin models. The values of h_{eff} as a function of $\bar{q}$ for the materials for which tests were conducted only in the ceramic-heated jet are shown in figure 8.

Motion-Picture Observations

Examination of the color motion pictures and the models tested in the ceramic-heated jet indicated that all the Teflon models acted in essentially the same manner. The Teflon surface was slick; there were no visible signs of vapor, flaming or melting, just a slow disappearance of the Teflon. The nylon, lucite, and polystyrene at approximately 2,200° F had a liquid film which appeared to extend for some distance rearward of the hemisphere-cylinder juncture. At approximately 3,800° F this liquid film appeared to vaporize downstream. The Haveg Rocketon and the resin models all acted somewhat similarly. At approximately 2,900° F and 3,800° F the noses of the models glowed brightly and liquid appeared to be coming from the nose and gradually vaporizing as it moved downstream along the sides of the models. The two inorganic salts, ammonium chloride and sodium carbonate, acted in the same manner as the Teflon. There were no visible signs of flaming or melting or glowing of the surfaces, just a slow disappearance of the material for about 5 to 6 seconds for the ammonium chloride and for about 3 to 4 seconds for the sodium carbonate. The models began to break up after these times. All the other materials exhibited good strength characteristics; however, very minute fractures sometimes developed into large cracks during the test, particularly for the Haveg Rocketon models. Figure 9 shows some typical models after testing.

The color motion pictures of the arc-jet tests indicated no change in the manner in which ablation occurred on the Teflon as compared with the models tested in the ceramic-heated jet. The nylon model did not show any clear-cut liquid film, but the nose surface was slick in appearance and there may have been some film. The Rocketon model appeared to vaporize.

The motion pictures indicated that during the tests in the ceramic-heated jet noticeable ablation did not start instantly for the Teflon and nylon models. There was a lag time of approximately 0.7 second for the

Teflon at a value of $\bar{q}$ of 76 Btu/ft^2-sec. This lag time decreased to about 0.3 second at a value of $\bar{q}$ of approximately 200 Btu/ft^2-sec.

The nylon lag times ranged from approximately 0.2 second at a value of $\bar{q}$ of 110 Btu/ft^2-sec to slightly less than 0.1 second at a value of $\bar{q}$ of 230 Btu/ft^2-sec. These lag times are due possibly to a finite time requirement, in practical cases, for the surface to reach a temperature at which melting or sublimation will occur. Motion pictures of tests in the arc jet show no lag times for the materials tested.

SUMMARY OF RESULTS

The ablation rates and the effective heats of ablation were evaluated for a number of materials in supersonic ceramic-heated and electric-arc-powered air jets for stagnation temperatures ranging from 2,000° F to 11,000° F. The average heat fluxes ranged from 20 to 1,570 Btu/ft^2-sec. The following results were obtained:

1. All the materials tested indicated effective heats of ablation ranging from 7 to 40 times greater than the useful heat absorption of a copper heat sink not undergoing ablation.

2. For Teflon, nylon, and Rocketon, which were tested over the complete range of heating rates, the results indicated that the effective heats of ablation would increase with increasing heating rates.

3. For several glass-reinforced phenolic-resin models, of which the resin content varied from 27 percent to 65 percent, the effective heats of ablation, for the same aerodynamic heat flux, decreased with increased resin content.

4. The inorganic salts, ammonium chloride and sodium carbonate from which models were constructed by cold-pressing of crystals did not compare well with the other materials with regard to strength; however, these models did show the highest values of effective heats of ablation at comparable aerodynamic heat fluxes, in comparison with the other materials tested.

Langley Aeronautical Laboratory,
National Advisory Committee for Aeronautics,
Langley Field, Va., May 5, 1958.

REFERENCES

1. Stalder, Jackson R.: The Useful Heat Capacity of Several Materials for Ballistic Nose-Cone Construction. NACA TN 4141, 1957.

2. Rashis, Bernard: Exploratory Investigation of Transpiration Cooling of a 40° Double Wedge Using Nitrogen and Helium as Coolants at Stagnation Temperatures of 1,295° to 2,910° F. NACA RM L57F11, 1957.

3. Modisette, Jerry L.: Preliminary Investigation of Lithium Hydride as a High-Temperature Internal Coolant. NACA RM L57F12a, 1957.

4. Rashis, Bernard: Preliminary Indications of the Cooling Achieved by Ejecting Water Upstream From the Stagnation Point of Hemispherical, 80° Conical, and Flat-Faced Nose Shapes at a Stagnation Temperature of 4,000° F. NACA RM L57I03, 1957.

5. Kinard, William H.: Feasibility of Nose-Cone Cooling by the Upstream Ejection of Solid Coolants at the Stagnation Point. NACA RM L57K22, 1958.

6. Casey, Francis W., Jr., and Hopko, Russell N.: Preliminary Investigation of Graphite, Silicon Carbide, and Several Polymer—Glass-Cloth Laminates in a Mach Number 2 Air Jet at Stagnation Temperatures of 3,000° F and 4,000° F. NACA RM L57K15, 1957.

7. Lees, Lester: Similarity Parameters for Surface Melting of a Blunt-Nosed Body in a High Velocity Gas Stream. Rep. No. GM-TM-184 (Contract No. AF 18(600)-1190), The Ramo-Wooldridge Corp., Guided Missile Res. Div., July 29, 1957.

8. Sutton, George W.: The Hydrodynamics and Heat Conduction of a Melting Surface. Jour. Aero. Sci., vol. 25, no. 1, Jan. 1958, pp. 29-32, 36.

9. Purser, Paul E., and Bond, Aleck C.: NACA Hypersonic Rocket and High-Temperature Jet Facilities. Rep. 140, AGARD, North Atlantic Treaty Organization (Paris), July 1957.

10. Hodgman, Charles D., ed.: Handbook of Chemistry and Physics. Thirty-sixth ed., Chemical Rubber Publishing Co., 1954-1955.

11. Fields, E. M., Hopko, Russell N., Swain, Robert L., and Trout, Otto F., Sr.: Behavior of Some Materials and Shapes in Supersonic Free Jets at Stagnation Temperatures up to 4,210° F, and Descriptions of the Jets. NACA RM L57K26, 1958.

TABLE I.- MATERIAL PROPERTIES

Material	Density, lb/cu ft	Thermal conductivity, Btu/ft-sec-°F	Specific heat, Btu/lb-°F (a)
Teflon	130	35.5×10^{-6}	0.3
Glass impregnated with 91-LD phenolic resin	115	41.7×10^{-6}	.23
41-percent phenolic resin	87.4	32×10^{-6}	.23
65-percent phenolic resin	100.1	32×10^{-6}	.23
44-percent phenolic resin	114.0	32×10^{-6}	.23
27-percent phenolic resin	132.7	32×10^{-6}	.23
37-percent phenolic resin	113.0	32×10^{-6}	.23
Phenolic nylon (57-percent phenolic)	73.6	32×10^{-6}	.23
Ammonium chloride	93	----------	----
Sodium carbonate	74.3	----------	----
Nylon	69.9	53.2×10^{-4}	.40
Polystyrene	66.1	25.2×10^{-4}	.32
Lucite	73.6	48.4×10^{-4}	.38

[a]All values of specific heat are for room temperature except that of Teflon, which is based on the average value from room temperature to approximately 600° F.

TABLE II.- SUMMARY OF TEST CONDITIONS

Model	Reinforcement	Configuration	T_t, °F	Surface pressure at stagnation point of model, lb/sq in. abs	Mach number	T_w, °F	$\bar{q}$	$\dot{w}/A$	h_{eff}
Teflon	None	A	2,243	75	2.0	1,000	75.8	0.02442	3,100
			2,840				116.3	.06760	1,721
			3,550				164.3	.10280	1,598
			3,755				178.2	.12140	1,468
		B	3,800	75			202.5	.14355	1,411
		E	10,880	70	1.9	1,000	157.0	.7695	2,091
41-percent phenolic resin	Refrasil	C	2,900	75	2.0	2,000	70.3	.0828	869
			3,800				140.2	.1078	1,412
27-percent phenolic resin	Glass cloth	C	2,895	75	2.0	2,000	70.3	.0568	1,238
			3,800				139.7	.0969	1,445
37-percent phenolic resin	Glass cloth	C	2,905	75	2.0	2,000	69.8	.0585	1,190
			3,800				139.7	.1027	1,364
44-percent phenolic resin	Glass cloth	C	2,930	75	2.0	2,000	71.8	.0836	1,048
			3,800				139.7	.1123	1,247
65-percent phenolic resin	Glass cloth	C	2,920	75	2.0	2,000	71.2	.0855	848
			3,800				139.7	.1222	1,147
Nylon	None	A	2,235	75	2.0	600	108.5	.09575	1,133
			3,745				225.5	.2348	947
Lucite	None	A	2,240	75	2.0	250	132	.05705	2,320
			3,810				251.5	.1878	1,342

TABLE II.- SUMMARY OF TEST CONDITIONS - Concluded

Model	Reinforcement	Configuration	T_t, °F	Surface pressure at stagnation point of model, lb/sq in. abs	Mach number	T_w, °F	$\bar{q}$	$\dot{w}/A$	h_{eff}
Polystyrene	None	A	2,280 3,755	75	2.0	250	134.8 248	0.07745 .1857	1,728 1,332
Haveg Rocketon	----------	A	2,280 3,800	75	2.0	2,000	18.6 127.3	.02840 .1216	652 1,045
Ammonium chloride	None	A	3,550 2,150	75	2.0	635	204.3 106	.05280 .03255	3,922 3,256
Sodium carbonate	None	A	3,550	75	2.0	1,560	139.2	.0518	2,662
Nylon	None	E	11,000	70	1.9	250	1,570	.5018	3,142
Haveg Rocketon	----------	E	11,000	70	1.9	2,000	1,550	.4298	3,615
Melamine resin M and C-5	Fine fiber glass	D	3,800	75	2.0	2,000	125.5	.137	1,000
Melamine resin GB-28M	Medium fiber glass	D	3,800	75	2.0	2,000	125.5	.165	771
Phenolic resin GB-125	Fine fiber glass	D	3,800	75	2.0	2,000	125.5	.123	1,362
Phenolic resin GB-261D	Coarse fiber glass	D	3,800	75	2.0	2,000	125.5	.218	739
Phenolic resin AA-13	Asbestos	D	3,800	75	2.0	2,000	125.5	.166	765

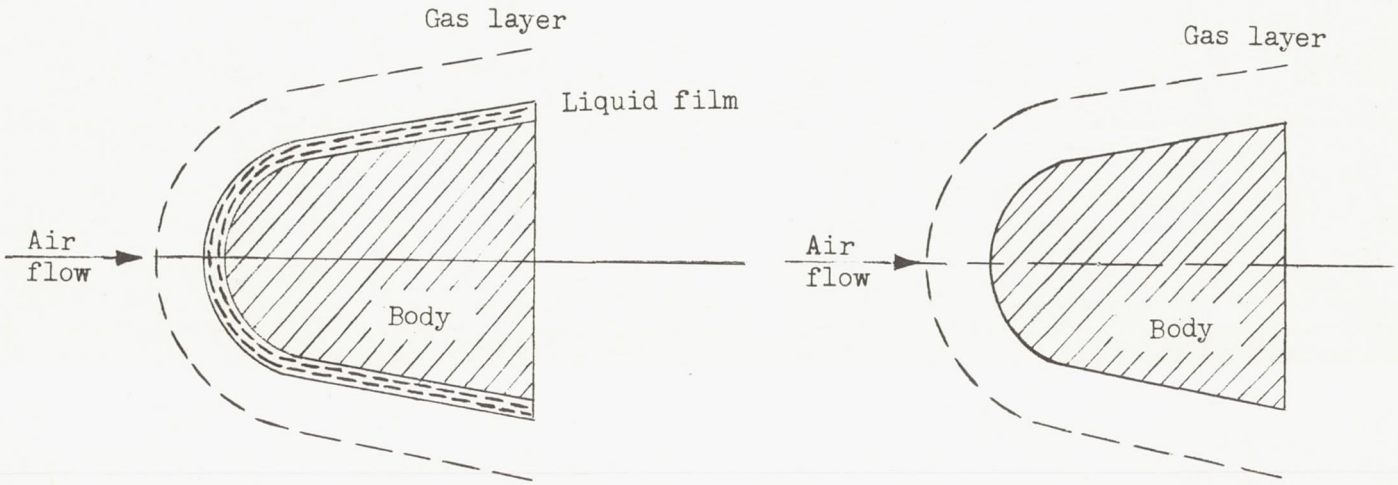

(a) Ablation by melting and vaporization.

(b) Ablation by sublimation.

Figure 1.- Schematic diagrams of two bodies undergoing ablation.

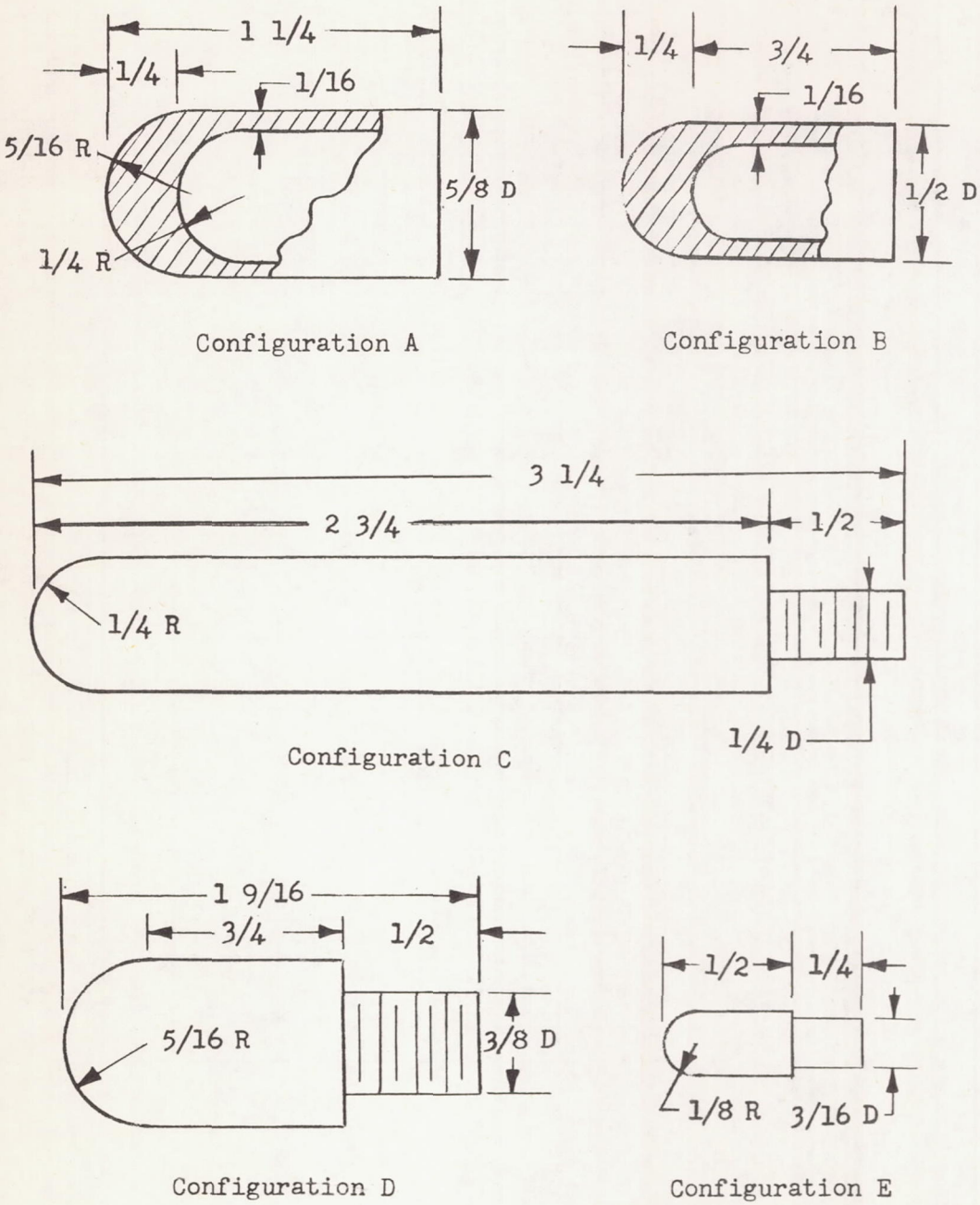

Figure 2.- Configurations tested.

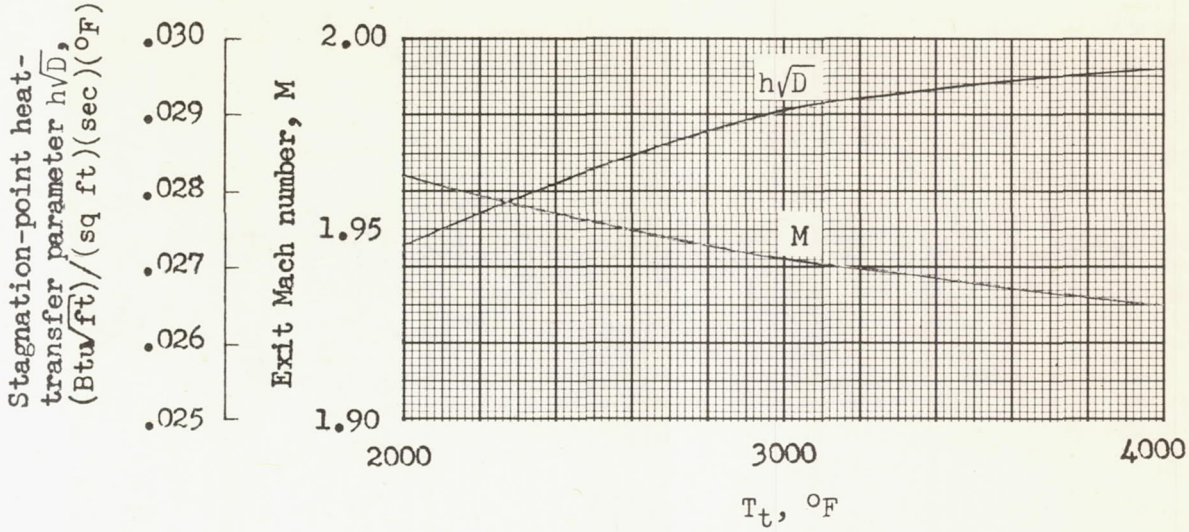

(a) Mach number and stagnation-point heat-transfer parameter.

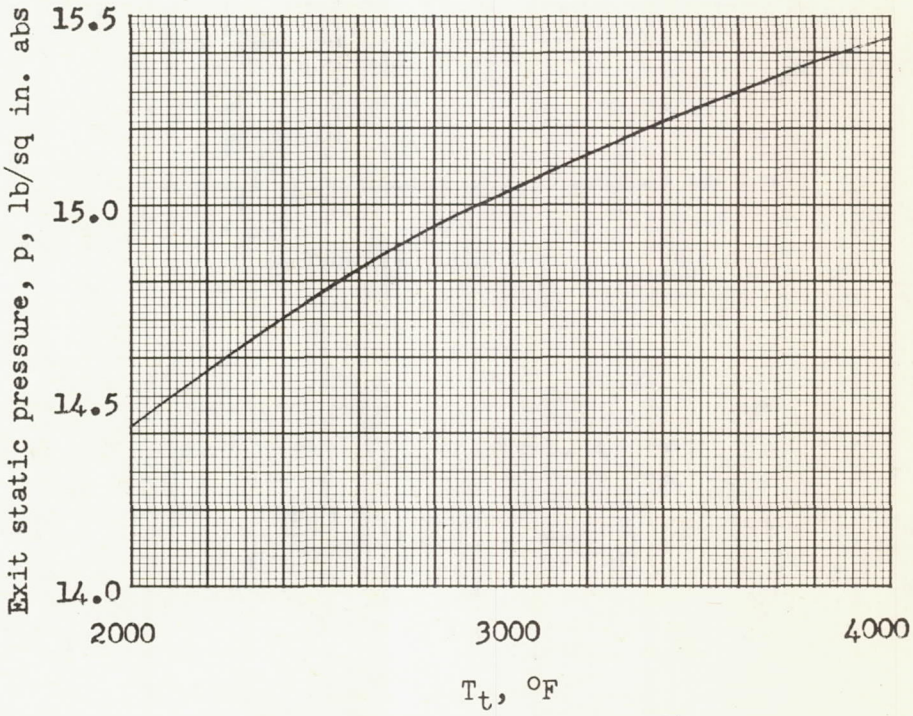

(b) Static pressure.

Figure 3.- Theoretical flow parameters for ceramic-heated jet (laboratory model).

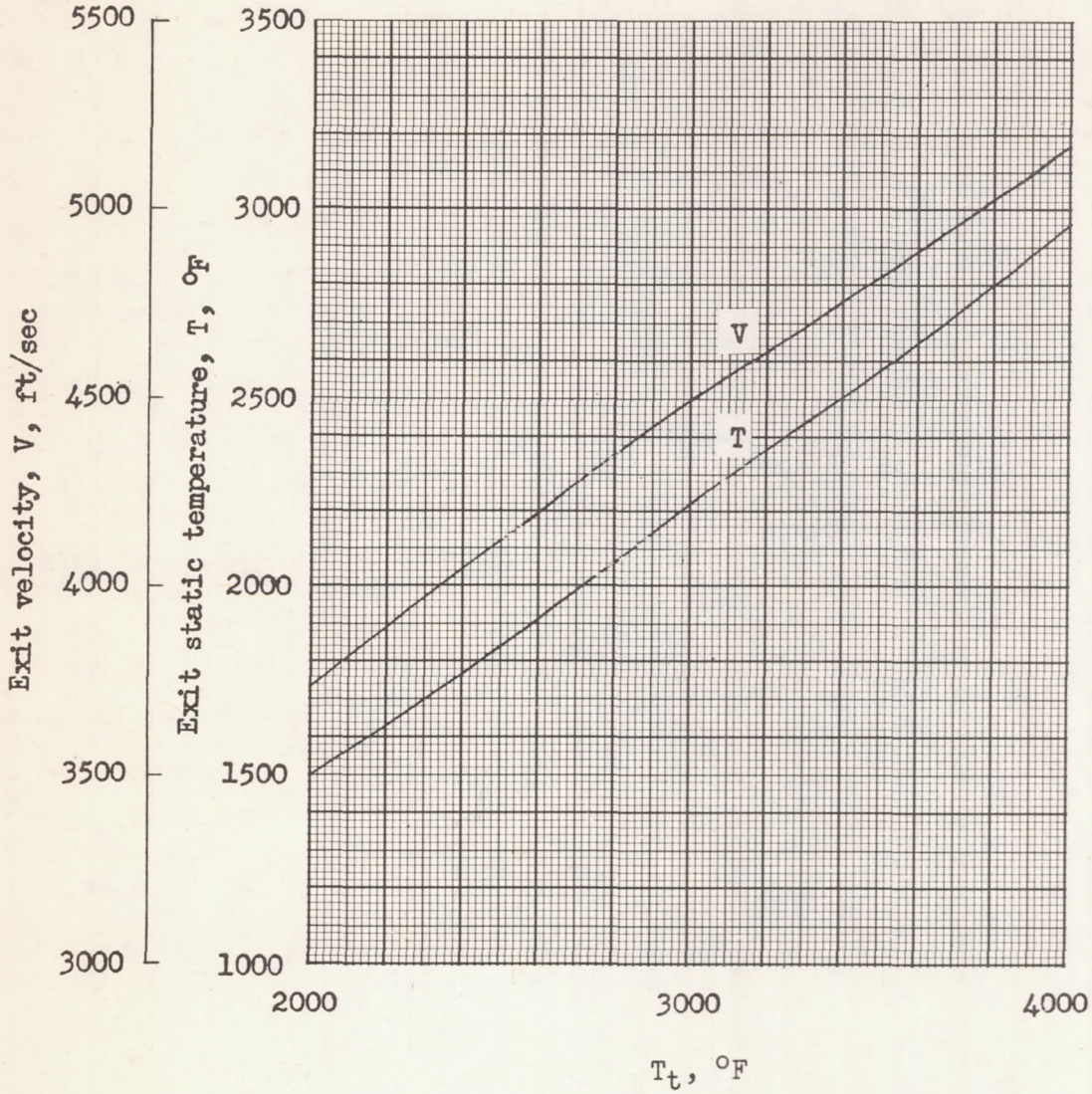

(c) Velocity and static temperature.

Figure 3.- Concluded.

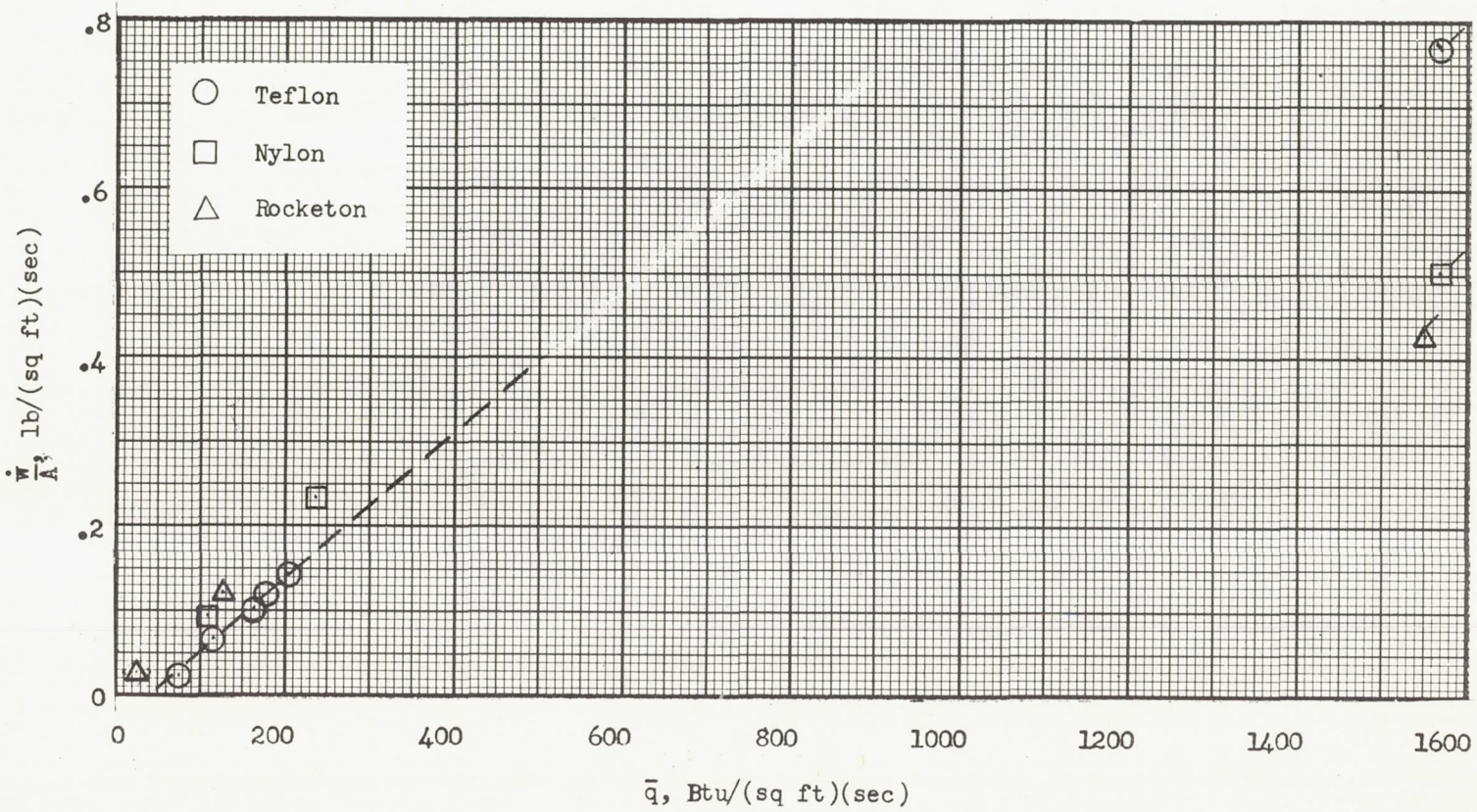

Figure 4.- Average ablation rate per unit area as function of average noseshape heat flux. Flagged symbols represent data obtained in electric-arc-powered air jet.

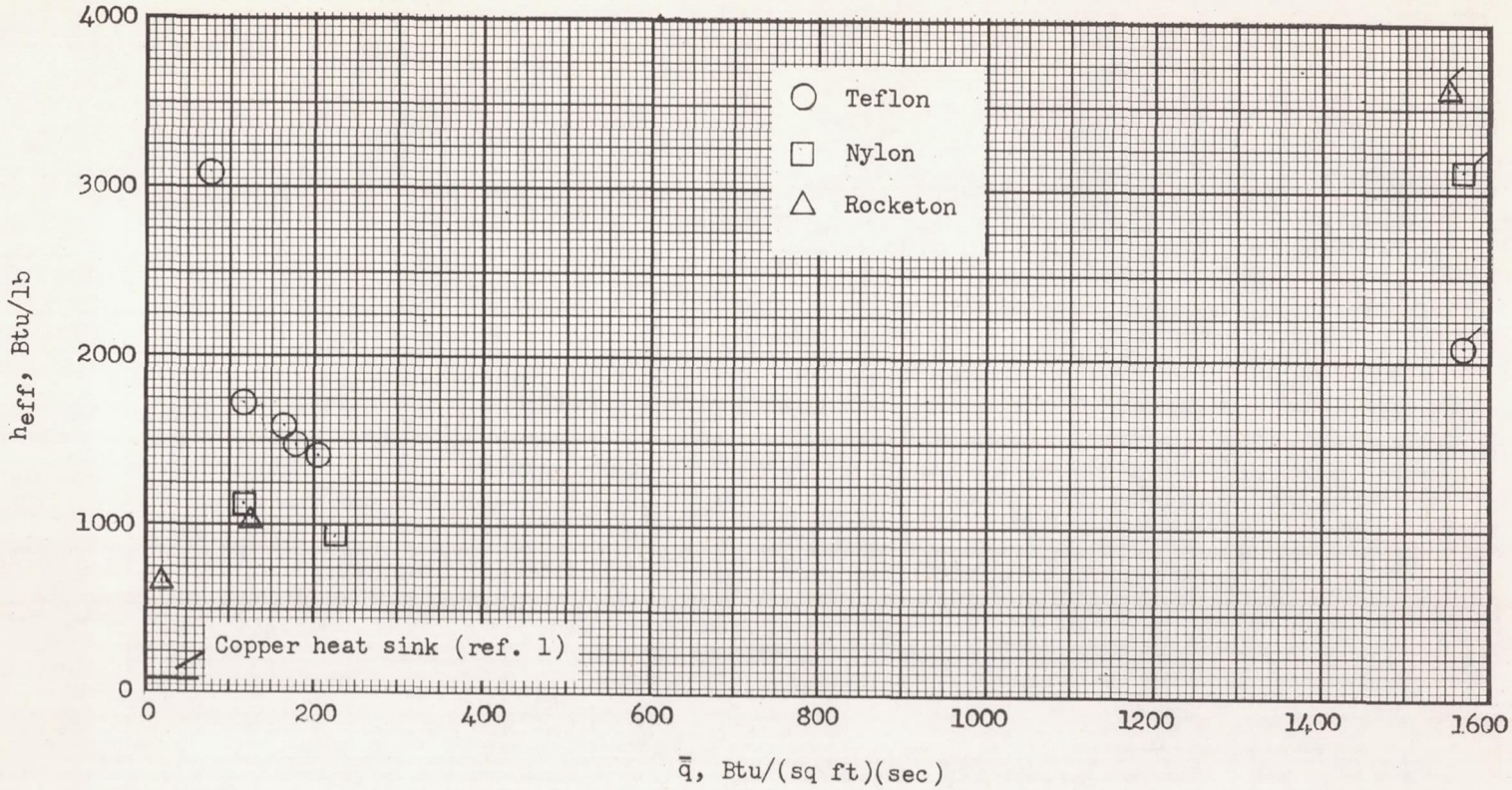

Figure 5.- Variation of effective heat of ablation with average nose-shape heat flux. Flagged symbols represent data obtained in electric-arc-powered air jet.

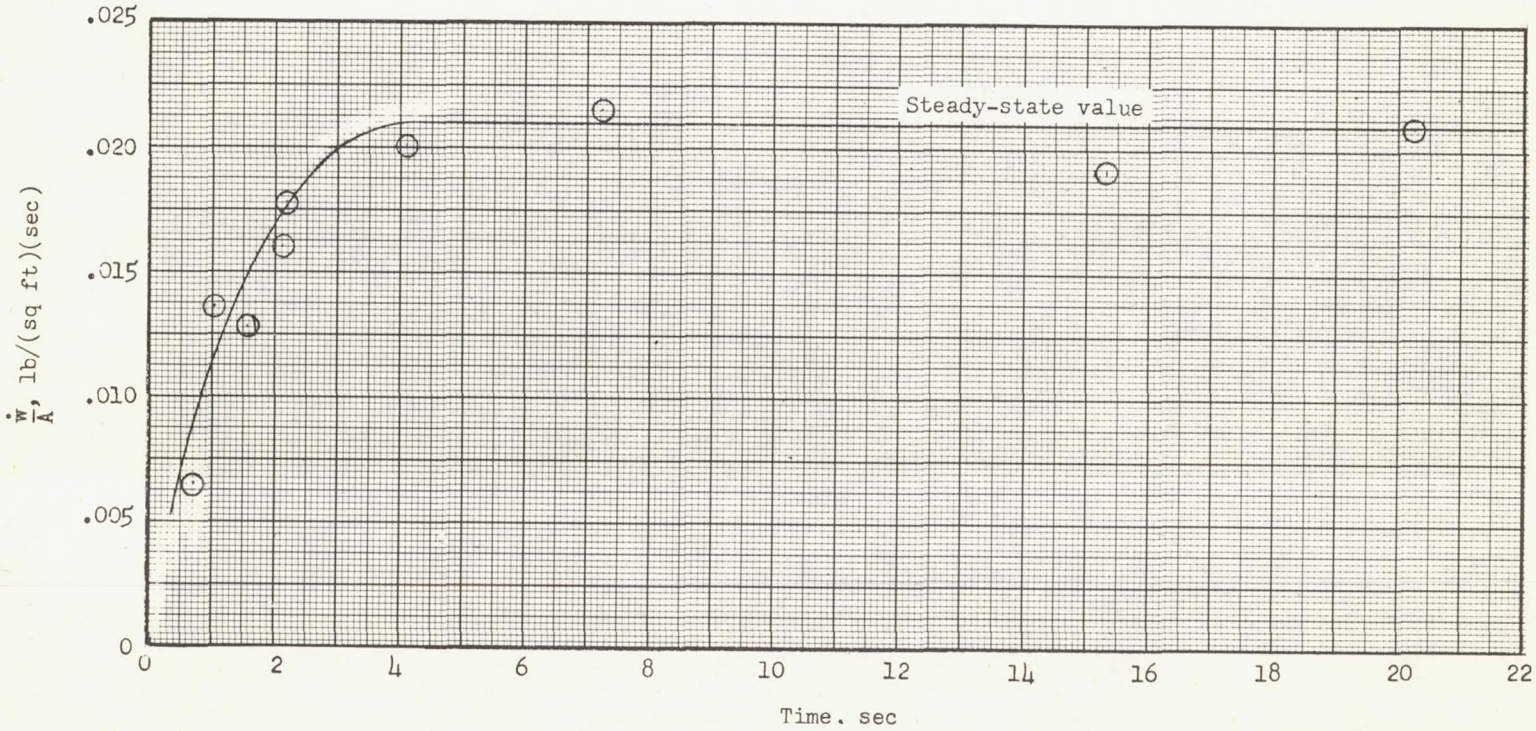

Figure 6.- Ablation rate for 5/8-inch-diameter-hemisphere Teflon model for $\overline{q}$ = 68 Btu/(sq ft)(sec).

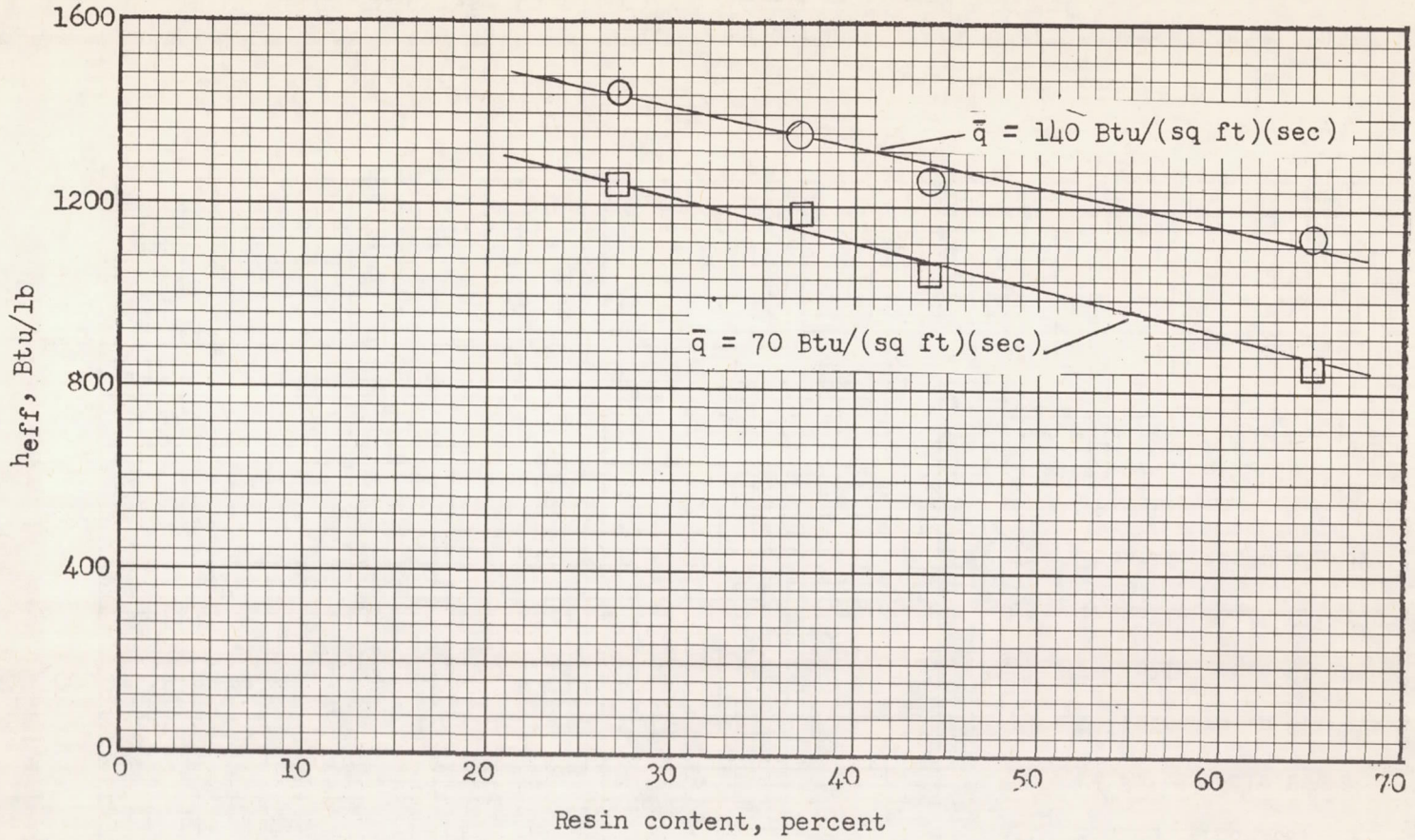

Figure 7.- Effect of resin content on effective heat of ablation of 1/2-inch-diameter hemispherical glass-reinforced phenolic-resin models.

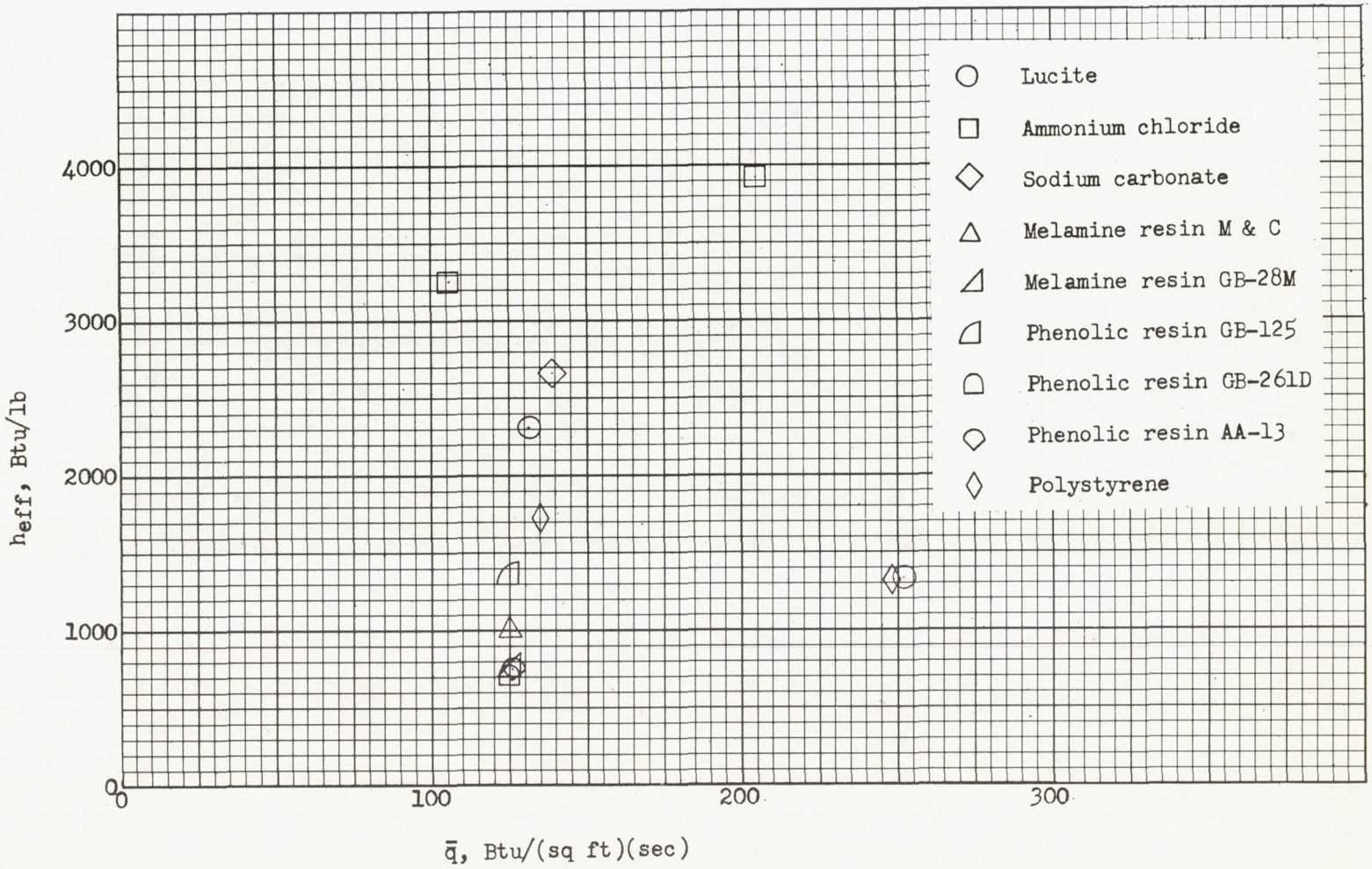

Figure 8.- Values of effective heat of ablation as a function of average aerodynamic heat flux for materials tested only in ceramic-heated air jet.

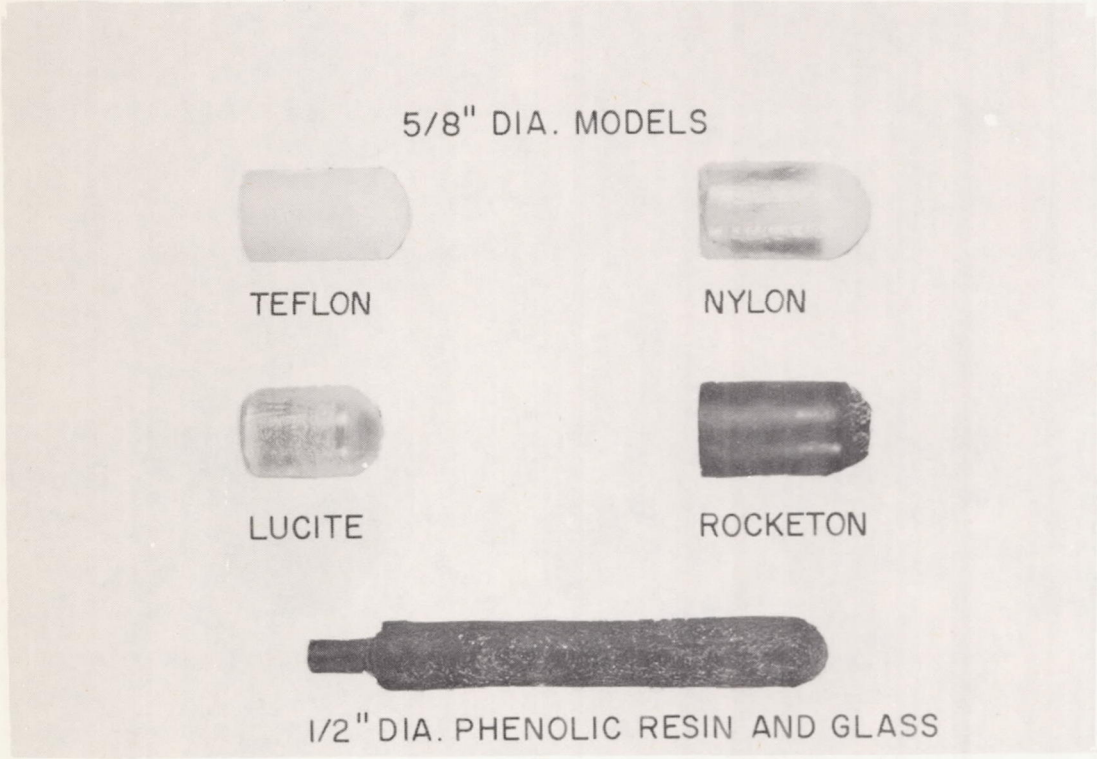

L-58-1671.1

Figure 9.- Models tested in ceramic-heated jet (laboratory model).